JACS
JOURNAL OF THE AMERICAN CHEMICAL SOCIETY
Cite This: J. Am. Chem. Soc. 2018, 140, 12715−12719
Communication
pubs.acs.org/JACS

Crystalline Dioxin-Linked Covalent Organic Frameworks from Irreversible Reactions

Bing Zhang,[†] Mufeng Wei,[†] Haiyan Mao,[‡] Xiaokun Pei,[†] Sultan A. Alshmimri,[§] Jeffrey A. Reimer,[‡] and Omar M. Yaghi*[,†,§]

[†]Department of Chemistry, University of California−Berkeley; Materials Sciences Division, Lawrence Berkeley National Laboratory; Kavli Energy NanoSciences Institute at Berkeley, and Berkeley Global Science Institute, Berkeley, California 94720, United States

[‡]Department of Chemical and Biomolecular Engineering, University of California−Berkeley, and Environmental Energy Technologies Division, Lawrence Berkeley National Laboratory, Berkeley, California 94720, United States

[§]UC Berkeley-KACST Joint Center of Excellence for Nanomaterials for Clean Energy Applications, King Abdulaziz City for Science and Technology, Riyadh 11442, Saudi Arabia

Supporting Information

ABSTRACT: Triangular 2,3,6,7,10,11-hexahydroxytriphenylene (HHTP) and linear tetrafluorophthalonitrile (TFPN) or 2,3,5,6-tetrafluoro-4-pyridinecarbonitrile (TFPC) were linked by 1,4-dioxin linkages to form crystalline 2D covalent organic frameworks, termed COF-316 and -318. Unlike the condensation reactions commonly used to crystallize the great majority of COFs, the reactions used in this report are based on nucleophilic aromatic substitution reactions (S_NAr) that are considered irreversible. Our studies show that the reactivity of TFPN and TFPC with HHTP is enhanced by the nitrile substituents leading to facile reactions of planar building units to yield the present 1,4-dioxin linked COFs. Because these reactions are irreversible, the resultant frameworks have high chemical stability in both acid and base. This has led to postsynthetic modifications of COF-316 by reactions necessitating extreme conditions to covalently install functionalities not otherwise accessible. We also report the permanent porosity of these COFs.

Reticular chemistry of covalent organic frameworks (COFs) represents the practice of organic chemistry in 2D and 3D, beyond discrete molecules (0D) and polymers (1D).[1,2] Realizing COFs in crystalline form has been an essential component to determining their structures on the atomic scale and ultimately to developing what is now a rapidly growing field.[3−9] Conventionally reversible covalent bond formation is needed for the crystallization of COFs, but it is this aspect that has intrinsically limited their high stability as it renders these materials chemically vulnerable.[10−12] To move COF chemistry beyond this dichotomy into a regime where irreversible bond formation also leads to crystalline products, we postulate it is necessary to develop linkage chemistry that obviates the common reliance on condensation reactions. Such pathways generally yield frameworks susceptible to hydrolysis, even though strategies such as tautomerization and linkage conversion have been applied to enhance framework stability.[13−16] In this report, we translate a common molecular organic reaction (Figure 1a), nucleophilic aromatic substitution (S_NAr), for the first time, into the realm of COFs. Specifically, we show how in the presence of base, 2,3,6,7,10,11-hexahydroxytriphenylene (HHTP) can react with tetrafluorophthalonitrile (TFPN) or 2,3,5,6-tetrafluoro-4-pyridinecarbonitrile (TFPC) to yield two crystalline, porous, dioxin-linked frameworks, COF-316 and -318, respectively (Figure 1b). The strong electron withdrawing substituents on the TFPN and TFPC building units make them prone to nucleophilic attack by the hydroxyl functionalities of HHTP (Figure 1c). Ring-closure by two consecutive S_NAr reactions yields an irreversible heteroaromatic dioxin linkage. Our success in crystallizing these COFs extends the scope of reticular synthesis to irreversible linkages. The impact of this advance is borne out in the fact that the stability of COF-316 in both strong acid and base allows its postsynthetic modification under extreme chemical conditions, and the covalent introduction of functionalities that were previously inaccessible.

We initially targeted the synthesis of a dioxin-linked molecular analog **1** (Figure 1a) in order to ascertain the planarity of the dioxin ring. The slow evaporation of acetonitrile solution of **1** produced crystals, which were analyzed by single crystal X-ray diffraction to reveal that the 1,4-dioxin ring is indeed coplanar with the fused phenyl rings. This was deemed essential in facilitating the stacking of the prospective 2D COF layer.[17] The irreversibility of the dioxin formation was probed by attempted exchange reactions of **1** with 4-methyl catechol. In these experiments, no exchanged product was observed by ^{1}H NMR (SI, figure S47).

With this knowledge in mind, we attempted the synthesis of COFs by reacting TFPN with HHTP as linear and triangular linkers, respectively. The strong electron withdrawing nitrile groups of TFPN are expected to enhance the electrophilicity of its C−F bond and therefore the reactivity toward HHTP. Extensive efforts were applied to screen various synthetic conditions including linkers, solvent mixtures, temperature and reaction time. A crystalline framework, termed COF-316, was successfully synthesized in the presence of stoichiometric

Received: August 6, 2018
Published: September 24, 2018

DOI: 10.1021/jacs.8b08374
J. Am. Chem. Soc. 2018, 140, 12715−12719

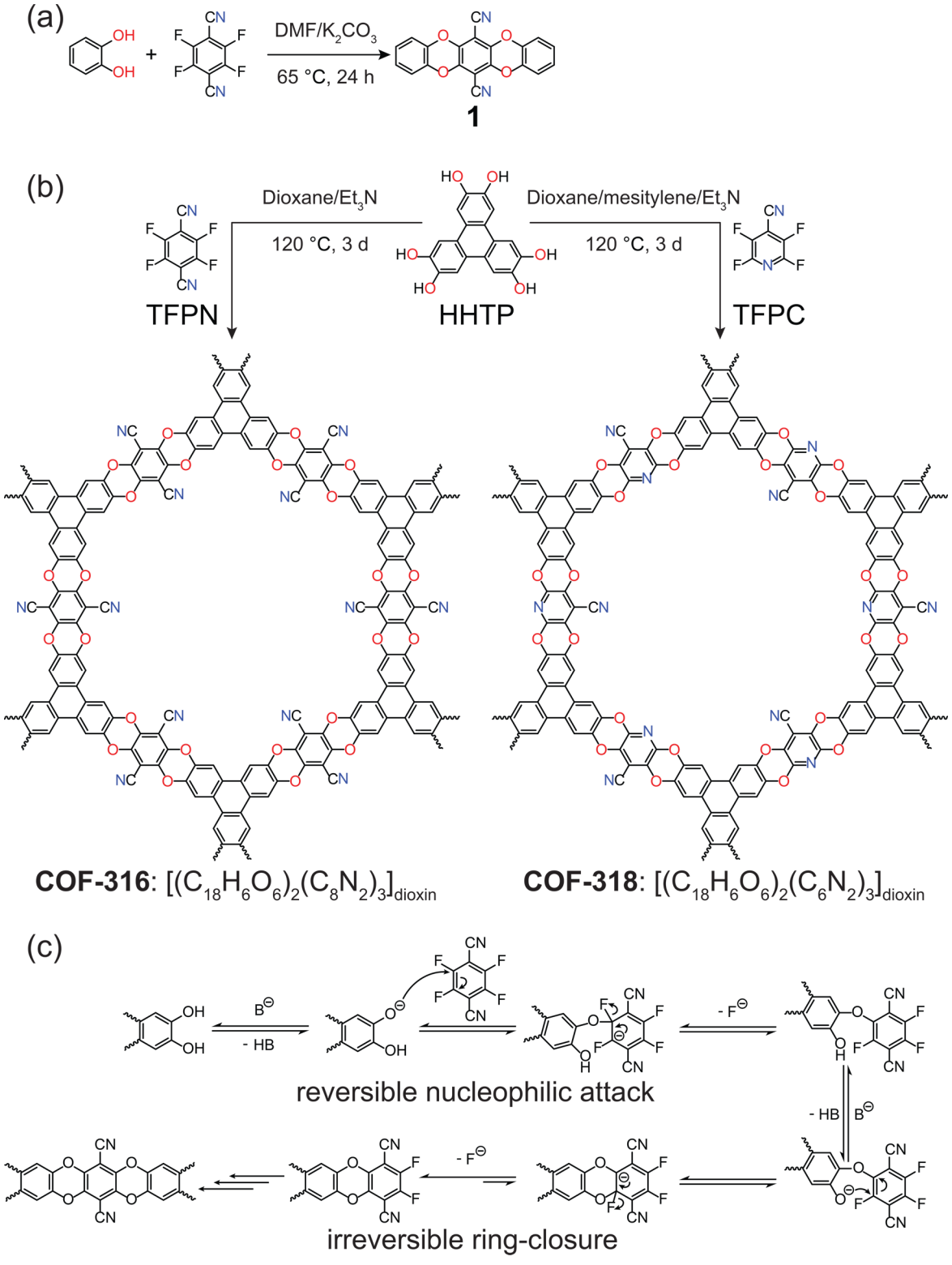

Figure 1. (a) Synthesis of molecular analog **1**. (b) Synthesis of COF-316 and -318. (c) Proposed mechanism of dioxin linkage formation.

triethylamine as base at 120 °C for 3 d in high yield (84%). We further extended the reaction scope by crystallizing COF-318 by linking HHTP and TFPC using similar conditions. We note that the synthetic conditions for these COFs are different from those used in making dioxin based polymers (soluble or amorphous).[18] It is remarkable that crystallinity of these COFs (Figure 2a,d, further discussed below) is achieved even though the dioxin ring-closure step is irreversible. We postulate that the rigidity of the building units and strong directionality of the linkage play an important role in enhancing the ordering of the structure. Moreover, the nitrile groups are indispensable for the reactivity of the nucleophilic substitution, as we found that weaker electron withdrawing groups such as trifluoromethyl and aldehyde substituents did not give complete reactions and

DOI: 10.1021/jacs.8b08374
J. Am. Chem. Soc. 2018, 140, 12715−12719

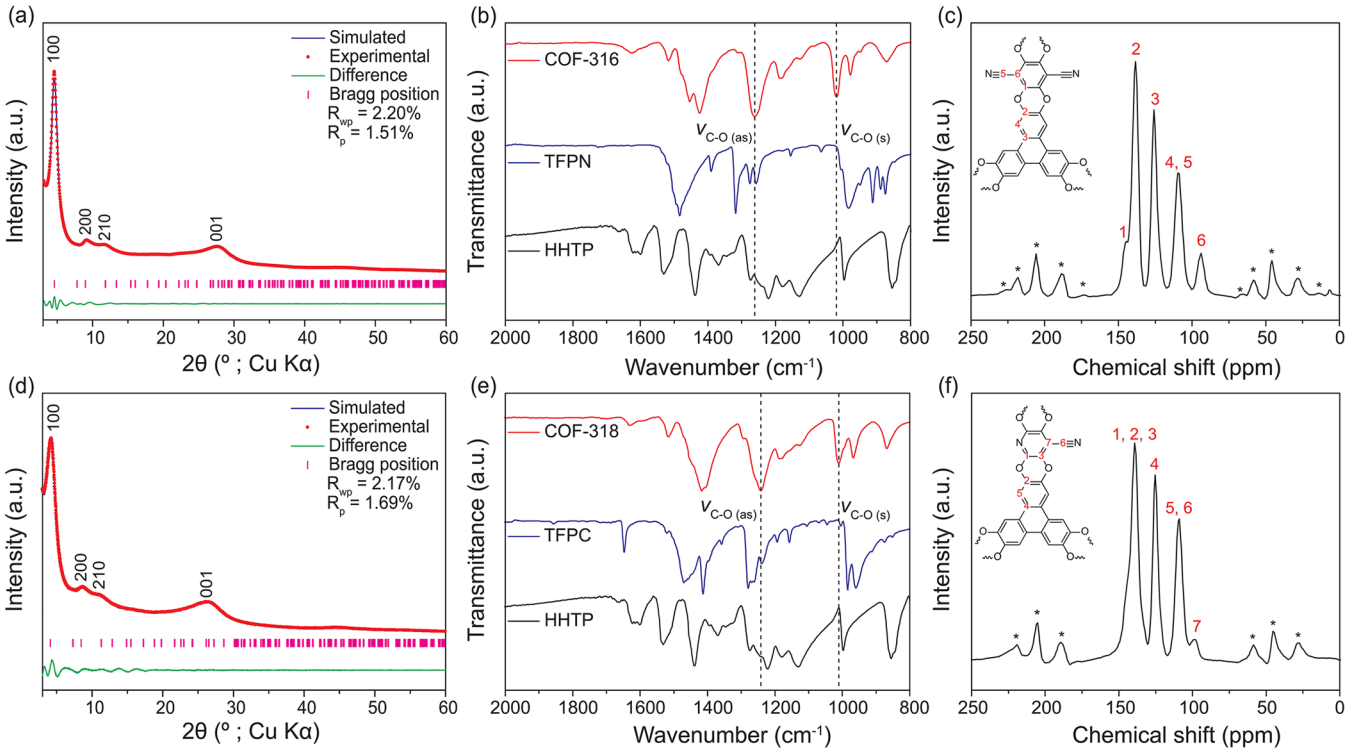

Figure 2. (a, d) PXRD patterns and Pawley refinement of COF-316 and -318, respectively. (b, e) FT-IR spectra of COF-316 and -318 compared with starting materials, respectively. (c, f) Solid state ^{13}C CP-MAS NMR spectra of COF-316 and -318, respectively. Asterisks denote the spinning sidebands.

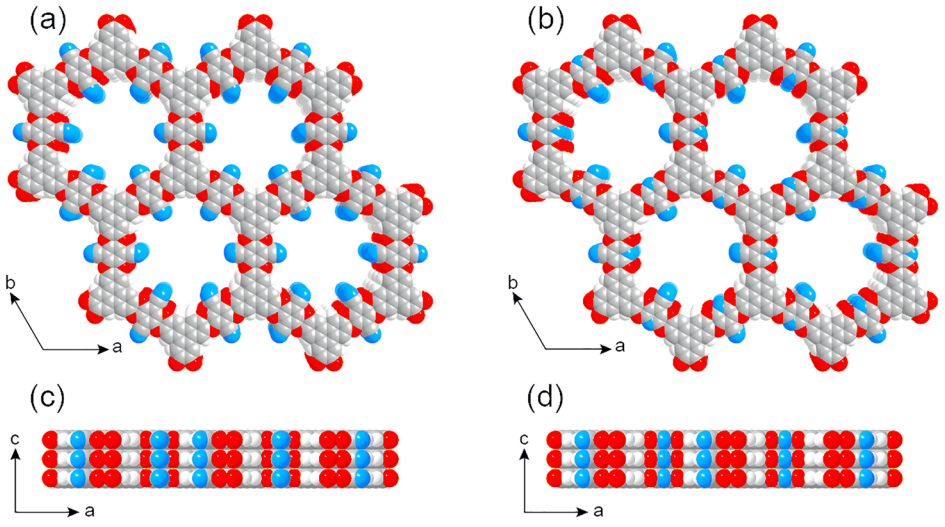

Figure 3. (a, b) Top views and (c, d) side views of the space-filling models of COF-316 and -318 in eclipsed stacking mode. Color code: H, white; C, gray; N; blue; O, red.

therefore no solid products (SI, table S1). Additionally, the dioxin-linked COFs can be crystallized under various conditions, demonstrating the robustness of the reaction (SI, table S1).

Both COF-316 and -318 were obtained as yellow microcrystalline powder, insoluble in common organic solvents such as acetone, alcohols, dichloromethane, tetrahydrofuran, *N*,*N*-dimethylformamide. Elemental analysis performed on the guest-free samples were in good agreement with the expected formulas of $[(C_{18}H_6O_6)_2(C_8N_2)_3]$ and $[(C_{18}H_6O_6)_2(C_6N_2)_3]$ for COF-316 and -318, respectively (SI, section S2). The solid-state UV−vis spectrum of COF-316 was similar to **1** but showed a red-shift in the absorbance peaks, possibly due to a higher degree of electron delocalization across and along the stacked planes (SI, section S13).[17]

The formation of C−O in the dioxin rings and the disappearance of the O−H in HHTP of COF-316 and -318 were confirmed by Fourier transform infrared (FT-IR) spectroscopy (Figure 2b,e; SI, section S4). The FT-IR spectra of COF-316 and -318 showed the characteristic dioxin C−O asymmetric and symmetric stretching modes at 1240 to 1262 and 1008 to 1020 cm^{-1}, respectively. These assignments were confirmed by the observation of analogous absorbance features in the FT-IR spectra of **1** (1246 and 1032 cm^{-1}). The O−H

DOI: 10.1021/jacs.8b08374
J. Am. Chem. Soc. 2018, 140, 12715−12719

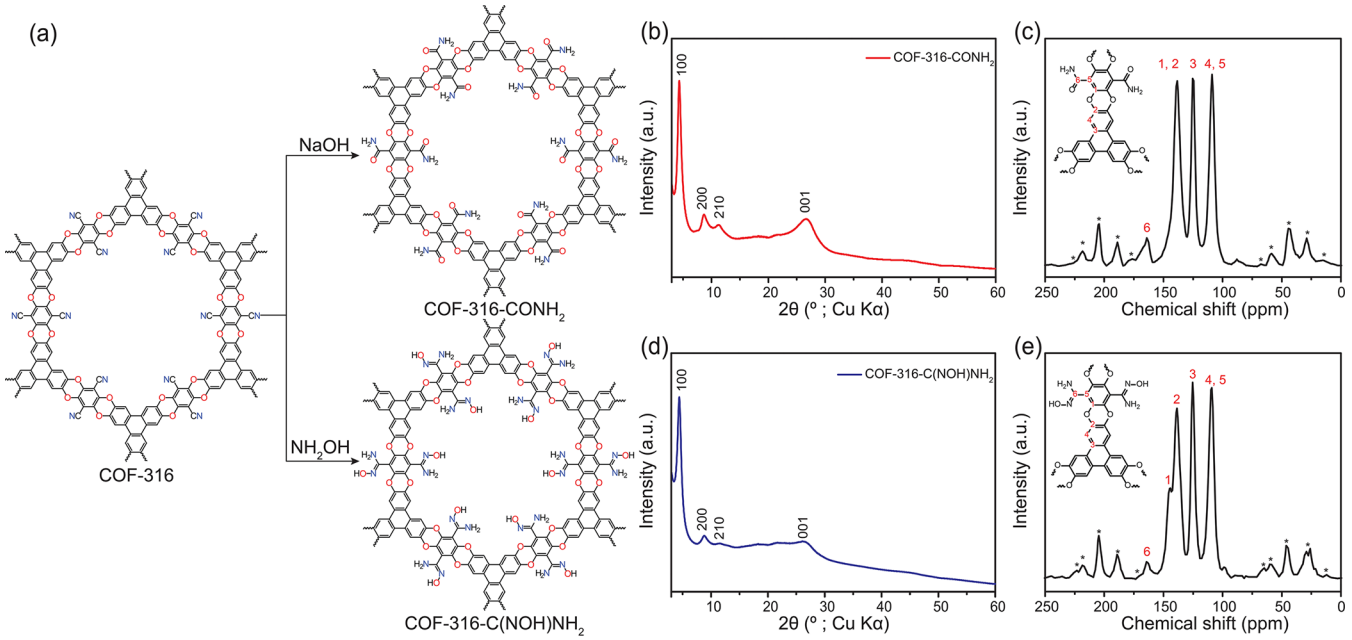

Figure 4. (a) Postsynthetic modification of COF-316. (b, d) PXRD patterns of COF-316-$CONH_2$ and -$C(NOH)NH_2$, indicating the retention of crystallinity and long-term stability in base. (c, e) Solid state ^{13}C CP-MAS NMR spectra of COF-316-$CONH_2$ and -$C(NOH)NH_2$, respectively. Asterisks denote the spinning sidebands.

stretching modes at 3200 to 3410 cm^{-1} in the HHTP starting material were not observed in the COF products. This indicated the conversion of − OH functional groups to C−O−C bond. A time dependent FT-IR analysis showed that the dioxin linkage is formed as early as 6 h into the reaction (SI, figure S5).

^{13}C cross-polarization magic angle spinning (CP-MAS) NMR spectroscopy further confirmed the formation of the dioxin linkages in the COFs. The ^{13}C CP-MAS NMR spectrum of COF-316 showed resonance signals at 139 and 146 ppm, which are characteristic of the C−O carbons. The signal at 95 ppm was assigned to aromatic carbons connected to nitriles, whereas those at 110 and 127 ppm were assigned to the nitrile carbons and aromatic carbons. Similarly, the ^{13}C CP-MAS spectrum of COF-318 can also be fully assigned (Figure 2c,f). All these assignments are done based on the chemical shifts of the corresponding carbon atoms in the starting building units (SI, section S5) and according to literature.[19]

The crystallinity of COF-316 and -318 was confirmed by powder X-ray diffraction (PXRD), with no diffraction peaks attributable to the starting materials (SI, section S6). The phase purity was confirmed by scanning electron microscopy: only one morphology was observed for each COF (SI, section S11). Given the planarity of the dioxin linkage and HHTP linkers, a 2D trigonal layered structure was expected to form when linking linear and trigonal building units (Figure 3). Therefore, eclipsed and staggered stacking modes were considered and models were built using Material Studio (SI, section S7). The powder pattern of COF-316 indicates three diffraction peaks at 4.47°, 9.08°, 11.72°, and a broad peak at 27.66°, corresponding to (100), (200), (210), and (001) reflection planes in both stacking modes, respectively. Pawley refinement was performed on the obtained powder pattern to afford unit cell parameters $a = b = 23.163(90)$ Å; $c = 3.163(12)$ Å with $R_{wp} = 2.20\%$ and $R_p = 1.51\%$. Likewise, the unit cell parameters of COF-318 can also be obtained by Pawley refinement (SI, section S6). A time dependent PXRD analysis shows that the immediately precipitated product is already crystalline (SI, figure S17). This shows that dioxin-linked COFs have distinct crystallization kinetics from imine-linked COFs where amorphous products are formed in the early stage of the reaction.[20] It is noteworthy that due to the limited number of peaks, it is not possible to unambiguously assign the framework to either eclipsed or staggered stacking mode. However, the porosity data facilitates the differentiation of these two modes, as discussed below.

N_2 adsorption analysis was performed after removal of guest molecules from the pores of the two frameworks by activation *in vacuo* (SI, section S8). The N_2 isotherms of COF-316 and -318 were measured at 77 K and were found to have characteristic Type I shape, indicating microporosity of both COFs. Brunauer−Emmett−Teller (BET) surface areas of COF-316 and -318 were calculated to be 557 and 576 $m^2 g^{-1}$, respectively. The pore size distribution of the structures was estimated using a quenched solid density functional theory model to fit the adsorption branch of the isotherms yielding estimated pore widths of 12 and 15 Å for COF-316 and -318. These values are in good agreement with the predicted values (12.7 and 15.2 Å) for an eclipsed stacking mode. Based on this finding, the stacking mode for each structure was assigned as eclipsed.

The thermal stability of COF-316 and -318 was evaluated using thermogravimetric analysis. Both COFs exhibited high thermal stability, showing no significant weight loss up to 400 °C under a N_2 atmosphere (SI, section S12). The chemical stability of COF-316 and -318 was also examined (SI, section S9) by treating the COFs with concentrated HCl (*aq.*) and NaOH (*aq.*) at room temperature. Comparison of FT-IR spectra and PXRD patterns of COF-316 and -318 before and after treatment in 12 M HCl (*aq.*) for 3 d demonstrated the long-term integrity of the dioxin linkages and full retention of crystallinity (SI, section S9). Moreover, N_2 adsorption analysis shows almost no decrease in BET surface area of the acid- and base-treated COFs (SI, figure S26,S29). In fact, the BET

DOI: 10.1021/jacs.8b08374
J. Am. Chem. Soc. 2018, 140, 12715−12719

surface area of COF-318 increased by 34%, after the acid treatment. We speculate that this is due to the fact that acid reacts with and removes the remaining pyridine-containing oligomers in the pores from COF synthesis.

Interestingly, during stability tests the nitriles on the backbone of COF-316 were partially converted to amides under strongly basic conditions (6 M NaOH), as evidenced by the emergence of an amide C═O stretching at 1679 cm^{-1} in the FT-IR (SI, figure S25). The chemical stability of COFs under extreme conditions previously limited the scope of reactions that can be employed in postsynthetic modifications,[21] however, this does not appear to be the case for these dioxin-linked COFs. Therefore, we probed the scope of this reactivity by performing postsynthetic modification reactions on COF-316. Two new functionalities, amide and amidoxime, which can potentially be applied to uranium sequestration,[22] were successfully introduced into COFs, for the first time, by nitrile hydrolysis in concentrated NaOH (*aq.*) and nucleophilic attack by hydroxylamine, respectively. PXRD patterns showed that COF-316-$CONH_2$ and COF-316-$C(NOH)NH_2$ fully retained their crystallinity (Figure 4b,d). The conversions of nitriles were monitored by FT-IR and ^{13}C CP-MAS NMR (SI, section S10; Figure 4c,e). Thus, the utility of the dioxin linkage is highlighted here by these two new postsynthetic modification reactions that both require high chemical stability.

In summary, we have synthesized two crystalline, porous COFs with new dioxin linkages using irreversible nucleophilic aromatic substitution reactions (S_NAr). The resulting high stability of the dioxin linkage allowed two new functionalities which were previously inaccessible, to be covalently introduced in COFs by postsynthetic modification under extreme conditions. This strategy opens up a new pathway for the design and construction of COFs with enhanced properties.

■ ASSOCIATED CONTENT

Supporting Information

The Supporting Information is available free of charge on the ACS Publications website at DOI: 10.1021/jacs.8b08374.

Crystallographic data (CIF)

Synthetic procedures, FT-IR, NMR, PXRD, SCXRD, porosity analysis, stability test, and postsynthetic modification data (PDF)

■ AUTHOR INFORMATION

Corresponding Author

*yaghi@berkeley.edu

ORCID

Bing Zhang: 0000-0001-8350-8624

Jeffrey A. Reimer: 0000-0002-4191-3725

Omar M. Yaghi: 0000-0002-5611-3325

Notes

The authors declare no competing financial interest.

■ ACKNOWLEDGMENTS

Support for the synthesis by King Abdulaziz City for Science and Technology (Center of Excellence for Nanomaterials and Clean Energy Applications) and the characterization of compounds by the Center for Gas Separations Relevant to Clean Energy Technologies, an Energy Frontier Research Center funded by the U.S. Department of Energy, Office of Science, Basic Energy Sciences under Award DE-SC0001015. Work performed at the Advanced Light Source (beamline 7.3.3 and 12.2.1) and at the Molecular Foundry is supported by the Director, Office of Science, Office of Basic Energy Sciences, of the U.S. Department of Energy under Contract DE-AC02-05CH11231. B.Z. acknowledges Dr. C. Zhu and Mr. Y. Cao for synchrotron X-ray diffraction data acquisition support, Mr. X. Gao for SEM image acquisition, Dr. C.S. Diercks, Mr. K.E. Cordova, Mr. P.J. Waller, Mr. K. Chakarawet and Mr. R.W. Flaig for helpful discussion.

■ REFERENCES

(1) Côte, A. P.; Benin, A. I.; Ockwig, N. W.; O'Keeffe, M.; Matzger, A. J.; Yaghi, O. M. *Science* **2005**, *310* (5751), 1166−1170.

(2) El-Kaderi, H. M.; Hunt, J. R.; Mendoza-Cortes, J. L.; Côte, A. P.; Taylor, R. E.; O'Keeffe, M.; Yaghi, O. M. *Science* **2007**, *316* (5822), 268−272.

(3) Ma, T.; Kapustin, E. A.; Yin, S. X.; Liang, L.; Zhou, Z.; Niu, J.; Li, L. H.; Wang, Y.; Su, J.; Li, J.; Wang, X.; Wang, W. D.; Wang, W.; Sun, J.; Yaghi, O. M. *Science* **2018**, *361* (6397), 48−52.

(4) Diercks, C. S.; Yaghi, O. M. *Science* **2017**, *355* (6328), No. eaal1585.

(5) Zhang, Y.-B.; Su, J.; Furukawa, H.; Yun, Y.; Gándara, F.; Duong, A.; Zou, X.; Yaghi, O. M. *J. Am. Chem. Soc.* **2013**, *135* (44), 16336−16339.

(6) Lin, S.; Diercks, C. S.; Zhang, Y.-B.; Kornienko, N.; Nichols, E. M.; Zhao, Y.; Paris, A. R.; Kim, D.; Yang, P.; Yaghi, O. M.; Chang, C. J. *Science* **2015**, *349* (6253), 1208−1213.

(7) Jackson, K. T.; Reich, T. E.; El-Kaderi, H. M. *Chem. Commun.* **2012**, *48* (70), 8823−8825.

(8) Baldwin, L. A.; Crowe, J. W.; Pyles, D. A.; McGrier, P. L. *J. Am. Chem. Soc.* **2016**, *138* (46), 15134−15137.

(9) Wei, P.-F.; Qi, M.-Z.; Wang, Z.-P.; Ding, S.-Y.; Yu, W.; Liu, Q.; Wang, L.-K.; Wang, H.-Z.; An, W.-K.; Wang, W. *J. Am. Chem. Soc.* **2018**, *140* (13), 4623−4631.

(10) Uribe-Romo, F. J.; Hunt, J. R.; Furukawa, H.; Klöck, C.; O'Keeffe, M.; Yaghi, O. M. *J. Am. Chem. Soc.* **2009**, *131* (13), 4570−4571.

(11) Lanni, L. M.; Tilford, R. W.; Bharathy, M.; Lavigne, J. J. *J. Am. Chem. Soc.* **2011**, *133* (35), 13975−13983.

(12) Li, H.; Li, H.; Dai, Q.; Li, H.; Brédas, J.-L. *Adv. Theory Simulations* **2018**, *1* (2), 1700015.

(13) Kandambeth, S.; Mallick, A.; Lukose, B.; Mane, M. V.; Heine, T.; Banerjee, R. *J. Am. Chem. Soc.* **2012**, *134* (48), 19524−19527.

(14) Dalapati, S.; Jin, S.; Gao, J.; Xu, Y.; Nagai, A.; Jiang, D. *J. Am. Chem. Soc.* **2013**, *135* (46), 17310−17313.

(15) Uribe-Romo, F. J.; Doonan, C. J.; Furukawa, H.; Oisaki, K.; Yaghi, O. M. *J. Am. Chem. Soc.* **2011**, *133* (30), 11478−11481.

(16) Guo, J.; Xu, Y.; Jin, S.; Chen, L.; Kaji, T.; Honsho, Y.; Addicoat, M. A.; Kim, J.; Saeki, A.; Ihee, H.; Seki, S.; Irle, S.; Hiramoto, M.; Gao, J.; Jiang, D. *Nat. Commun.* **2013**, *4* (1), 1−8.

(17) Vyas, V. S.; Haase, F.; Stegbauer, L.; Savasci, G.; Podjaski, F.; Ochsenfeld, C.; Lotsch, B. V. *Nat. Commun.* **2015**, *6* (1), 8508.

(18) McKeown, N. B.; Budd, P. M. *Chem. Soc. Rev.* **2006**, *35* (8), 675−683.

(19) Vile, J.; Carta, M.; Bezzu, C. G.; McKeown, N. B. *Polym. Chem.* **2011**, *2* (10), 2257−2260.

(20) Smith, B. J.; Overholts, A. C.; Hwang, N.; Dichtel, W. R. *Chem. Commun.* **2016**, *52* (18), 3690−3693.

(21) Waller, P. J.; Lyle, S.; Osborn Popp, T.; Diercks, C. S.; Reimer, J. A.; Yaghi, O. M. *J. Am. Chem. Soc.* **2016**, *138* (48), 15519−15522.

(22) Sun, Q.; Aguila, B.; Earl, L. D.; Abney, C. W.; Wojtas, L.; Thallapally, P. K.; Ma, S. *Adv. Mater.* **2018**, *30* (20), 1705479.

DOI: 10.1021/jacs.8b08374
J. Am. Chem. Soc. 2018, 140, 12715−12719